Available online at www.sciencedirect.com
SCIENCE DIRECT®
Journal of Photochemistry and Photobiology A: Chemistry 162 (2004) 489–496
Journal of Photochemistry and Photobiology A:Chemistry
www.elsevier.com/locate/jphotochem

Photostability of a series of two-photon absorbing fluorene derivatives

Kevin D. Belfield [a,*], Mykhailo V. Bondar [b], Olga V. Przhonska [b], Katherine J. Schafer [a]

[a] *Department of Chemistry and CREOL/School of Optics, University of Central Florida, P.O. Box 162366, Orlando, FL 32816-2366, USA*
[b] *Institute of Physics, Prospect Nauki, 46, Kiev-28, Kiev 03028, Ukraine*

Received 25 June 2003; received in revised form 10 September 2003; accepted 22 September 2003

Abstract

The photochemical stability of a series of two-photon absorbing (TPA) fluorene derivatives was investigated in air- and N_2-saturated acetonitrile (ACN) at room temperature. The quantum yields of the photoreactions, Φ, were determined at various concentrations of the fluorene derivatives, oxygen concentration of the solvent, and irradiation wavelength. The absorption and fluorescence spectra of the photoproducts, corresponding to different excitation conditions, were analyzed. Photooxidation and electron transfer processes are proposed as photobleaching mechanisms for the fluorene derivatives in ACN. The relatively low photochemical quantum yields ($\Phi \sim 10^{-4}$) make the derivatives particularly promising for linear and nonlinear optical applications.

Keywords: Fluorene derivatives; Photochemical quantum yield; Photostability; Photooxidation

1. Introduction

Organic materials with strong nonlinear optical absorptivities are the subject of great interest owing to a wide variety of their potential applications including optical power limiting materials [1], two-photon fluorescence imaging [2], two-photon photodynamic cancer therapy [3] and microfabrication [4]. In particular, new fluorene derivatives [5–11] that exhibit high two-photon absorption (TPA) are promising for several of the applications mentioned above. For nearly all these applications, high stability against chemical and photochemical decomposition is required. There have been reports of fluorene and its derivatives as environmental pollutants [12,13]. The effect of solvent and substituent on the photooxidation of fluorene was investigated [14]. The results indicated that the rate of photooxidation was solvent dependent, and mainly due to the difference in the solubility of atmospheric oxygen in the solvent. The presence of –COOH and $–CH_2COOH$ groups at the nine position of fluorene decreased its photochemical and thermal stability. The photochemistry of fluorene at a silica gel/air interface was reported [15] and an electron transfer mechanism for the formation of fluorenone by direct photolysis of fluorene was proposed. In general, relatively little is known about the photochemical reactivity of fluorenes, even though a number of fluorene derivatives have potential use in nonlinear optical processes, particularly in two-photon fluorescence imaging. Therefore, the photochemical investigation of new TPA fluorene derivatives is important to understand their possible applications and limitations.

Over the last several years, we have witnessed an intense increase in the use of two-photon excitation of organic materials for a number of processes, including two-photon three-dimensional fluorescence imaging. Perhaps the Achilles' heel of organic materials in both linear and nonlinear optical applications has been their photostability, or more aptly their photoinstability. Joint efforts of Reinhardt (Air Force Research Laboratory), Prasad (SUNY-Buffalo), and our laboratory have identified and demonstrated the use of a number of fluorene derivatives that exhibit two-photon upconverted fluorescence. Herein, we wish to report results of a comprehensive investigation of the photochemical stability, particularly photooxidative stability, of a series of fluorene derivatives (with different electron-donating and electron-withdrawing substituents) that possess both high two-photon absorptivity and high fluorescence quantum yields, important parameters for two-photon fluorescent dyes. This type of study is critical in forging ahead in the design and use of similar organic compounds in linear and nonlinear optics.

* Corresponding author. Tel.: +1-407-823-1028; fax: +1-407-823-2252.
E-mail address: kbelfiel@mail.ucf.edu (K.D. Belfield).

1010-6030/$ – see front matter © 2004 Elsevier B.V. All rights reserved.
doi:10.1016/S1010-6030(03)00393-9

2. Experimental

We investigated the photochemical stability of (7-benzothiazol-2-yl-9,9-didecylfluoren-2-yl)-diphenylamine (**1**), 9, 9-didecyl-2,7-bis-(*N*,*N*-diphenylamino)fluorene (**2**), and {4-[2-(7-diphenylamino-9,9-diethylfluoren-2-yl)vinyl]phenyl} phosphoric acid diethyl ester (**3**), whose synthesis was described previously [5,6]. These compounds were investigated in air- and N_2-saturated acetonitrile (ACN) at room temperature under UV irradiation. Deoxygenated solutions were obtained by bubbling nitrogen through the solutions for 20 min. UV lamp UVGL-25 (maximum irradiation wavelength $\lambda_{irr} \approx 360$ nm; full width half maximum of the spectral distribution, $\Delta\lambda \approx 15$ nm; integral irradiation intensity $I_0 \approx 4\,mW/cm^2$), UV lamp ENF-260C ($\lambda_{irr} \approx 250$ nm; $\Delta\lambda \approx 2$ nm; $I_0 \approx 4\,mW/cm^2$), and Xe-lamp irradiation passed through the excitation monochromator of the PTI QuantaMaster spectrofluorimeter (240 nm $< \lambda_{irr} <$ 400 nm; $\Delta\lambda \approx$ 5–8 nm; $I_0 \approx$ 0.5–1.2 mW/cm^2) were used for the photochemical decomposition of compounds **1**–**3**. Fluorene solutions, with concentrations $C \approx (2-5) \times 10^{-5}$ M, were irradiated at the wavelengths $\lambda_{irr} \approx 360$ and $\lambda_{irr} \approx 250$ nm in the entire volume of a quartz cuvette 1 cm × 1 cm × 3.5 cm.

Quantum yields of the photoreactions, Φ, were determined by a previously described absorption method [16] and based on the temporal dependencies of the optical density, $D(\lambda, t)$, of the irradiated fluorene solutions. The value Φ was calculated by the following equation [16]:

$$\Phi = \frac{D_0 - D_T}{\varepsilon \times \int_\lambda \int_0^T I_0(\lambda) \times [1 - 10^{-D(\lambda,t)}] d\lambda\, dt}, \quad (1)$$

where D_0, D_T and ε are the initial and final optical density of the solution and extinction coefficient, respectively; $I_0(\lambda)$ is the spectral distribution of the UV lamp intensity; T is the total irradiation time. The absorption spectra of compounds **1**–**3** and their photoproducts were measured with a Cary-3 UV-Vis spectrophotometer. The fluorescence spectra of compounds **1**–**3** in ACN, the fluorescence and excitation spectra of their photochemical products (diluted solutions $C \leq 3 \times 10^{-6}$ M) and spectral distribution of the UV lamps, $I_0(\lambda)$, were recorded on the PTI QuantaMaster spectrofluorimeter. The integrated intensity of the UV lamp irradiation, $I_0 = \int_\lambda I_0(\lambda) d\lambda$, was measured with a Laserstar powermeter (Ophir Optronics Inc.) with sensitivity in the nanowatt range.

Quantum yields of the photoreactions of compounds **1**–**3,** at low concentrations ($C \leq 3 \times 10^{-6}$ M), were obtained by the fluorescence method previously described [16], which was based on the temporal measurements of the fluorescence intensity. The fluorene solution was placed in a microcuvette (0.1 cm × 0.1 cm × 1 cm) and the entire volume was irradiated with a Xe-lamp, after passing through the excitation monochromator of the PTI QuantaMaster spectrofluorimeter. In this case the quantum yield of the photoreaction can be calculated as [16]:

$$\Phi = \frac{1 - (F_T/F_0)}{I_0 \times \sigma(\lambda_{irr}) \times \int_0^T (F(t)/F_0) dt}, \quad (2)$$

where F_0 and F_T are the initial and final fluorescence intensity from the microcuvette, respectively; I_0 the irradiation intensity; $\sigma(\lambda_{irr})$ is the molecular absorption cross-section at λ_{irr}. In Eq. (2) it is assumed that optical density and fluorescence of the photochemical products of **1**–**3** were negligible in the spectral region of the observed fluorescence.

3. Results and discussion

The detailed photophysical characterization of fluorene derivatives **1**–**3** (Fig. 1) in ACN and other aprotic solvents was described previously [7]. The absorption and fluorescence spectra of compounds **1**–**3** in ACN are shown in Fig. 2. These compounds are characterized by high fluorescence quantum yields in ACN (0.9 ± 0.08 (**1**), 0.7 ± 0.1 (**2**), and 0.9 ± 0.08 (**3**)), which were nearly independent of the oxygen concentration in the solvent. The fluorescence spectra of unsymmetrical derivatives **1** and **3** exhibited a strong dependence on solvent polarity in contrast to the symmetrical fluorene derivative **2** [7].

In order to understand the major factors that contribute to the photodegradation of fluorene derivatives **1**–**3**, the quantum yields of the photoreactions were measured at different concentrations, irradiation wavelength, and oxygen concentration. These data are presented in Table 1. For the concentrations $C \sim (2-5) \times 10^{-5}$ M, the values of Φ were obtained from the time-dependent absorption spectra of **1**–**3** presented in Figs. 3–5 for $\lambda_{irr} \approx 360$ nm. The same spectra were

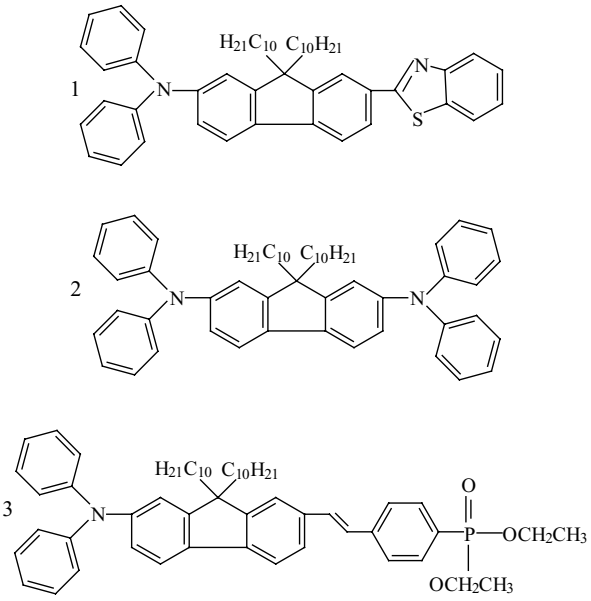

Fig. 1. Structures of compounds **1**–**3**.

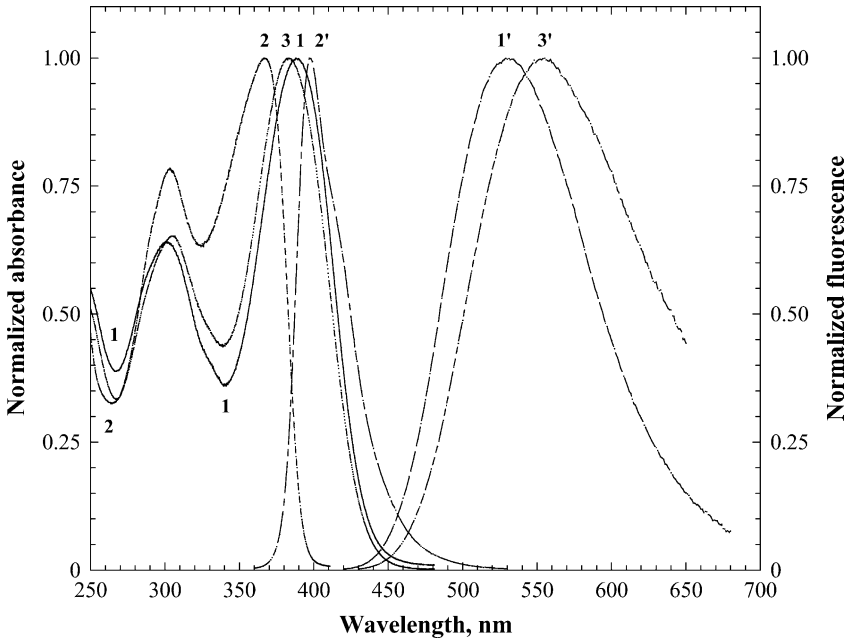

Fig. 2. Normalized absorption and fluorescence spectra of compounds **1** (1, 1′), **2** (2, 2′), and **3** (3, 3′) in ACN.

obtained for $\lambda_{irr} \approx 250$ nm and corresponding Φ are presented in Table 1. For low concentrations, $(1-3) \times 10^{-6}$ M, quantum yields of the photoreactions were measured by the fluorescence method mentioned above [16] for different λ_{irr} in the spectral region 240 nm $< \lambda_{irr} <$ 400 nm. Thus, the wavelength dependence quantum yields, $\Phi(\lambda_{irr})$ were obtained at low concentrations for **1–3** in ACN (Figs. 6–8). These experimental results facilitated a detailed photochemical analysis of **1**–**3**.

3.1. Analysis of **1**

Fluorene **1** undergoes complicated processes of photochemical decomposition. The quantum yield of the photoreaction of **1,** upon excitation in its main absorption band ($\lambda_{irr} \approx 360$ nm), increased with concentration essentially from $\Phi \approx 3 \times 10^{-5}$ ($C \approx 1.6 \times 10^{-6}$ M) to $\Phi \approx 3.5 \times 10^{-4}$ ($C \approx 2.4 \times 10^{-5}$ M), indicative of a second-order photoreaction. Deoxygenation of the solution at $C \approx 2.4 \times 10^{-5}$ M

Table 1
Quantum yields, Φ, of the photoreactions of **1**–**3** at different concentrations, C, excitation wavelength, λ_{exc}, and oxygen content in ACN.

N/N	Fluorene **1**	Fluorene **2**	Fluorene **3**
Φ	$(3.5 \pm 0.6) \times 10^{-4}$	$(6.5 \pm 1) \times 10^{-4}$	$(3.9 \pm 0.7) \times 10^{-4}$
λ_{exc} (nm)	360	360	360
air-saturated C (M)	2.4×10^{-5}	4.5×10^{-5}	2.5×10^{-5}
Φ	$(2.3 \pm 0.4) \times 10^{-4}$	$(6.5 \pm 1) \times 10^{-4}$	$(1.7 \pm 0.3) \times 10^{-4}$
λ_{exc} (nm)	250	250	250
air-saturated C (M)	2.4×10^{-5}	4.5×10^{-5}	2.5×10^{-5}
Φ	$(2.7 \pm 0.4) \times 10^{-6}$	$(1.8 \pm 0.3) \times 10^{-4}$	$(1.6 \pm 0.3) \times 10^{-5}$
λ_{exc} (nm)	360	360	360
N_2-saturated C (M)	2.4×10^{-5}	4.5×10^{-5}	2.5×10^{-5}
Φ	$(6.3 \pm 1) \times 10^{-6}$	$(5 \pm 0.8) \times 10^{-4}$	$(5.8 \pm 1) \times 10^{-5}$
λ_{exc} (nm)	250	250	250
N_2-saturated C (M)	2.4×10^{-5}	4.5×10^{-5}	2.5×10^{-5}
Φ	$(3 \pm 1) \times 10^{-5}$	$(6.5 \pm 1.5) \times 10^{-5}$	$(2.3 \pm 0.6) \times 10^{-4}$
λ_{exc} (nm)	360	360	360
air-saturated C (M)	1.6×10^{-6}	2.4 x 10^{-6}	1.6×10^{-6}
Φ	$(1.2 \pm 0.5) \times 10^{-5}$	$(3.5 \pm 1) \times 10^{-5}$	$(6 \pm 1.5) \times 10^{-5}$
λ_{exc} (nm)	250	250	250
air-saturated C (M)	1.6×10^{-6}	2.4×10^{-6}	1.6×10^{-6}

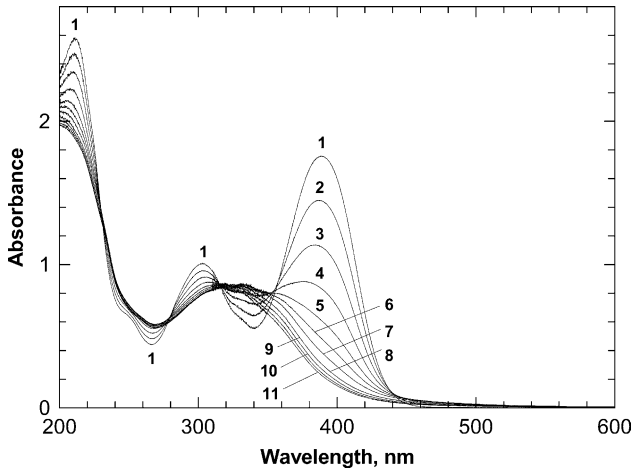

Fig. 3. Time-dependent absorption spectra of **1** in ACN ($\lambda_{irr} = 360$ nm; $I_0 = 4$ mW/cm^2): (1) 0 min; (2) 15 min; (3) 30 min; (4) 45 min; (5) 60 min; (6) 75 min; (7) 90 min; (8) 120 min; (9) 150 min; (10) 180 min; and (11) 210 min.

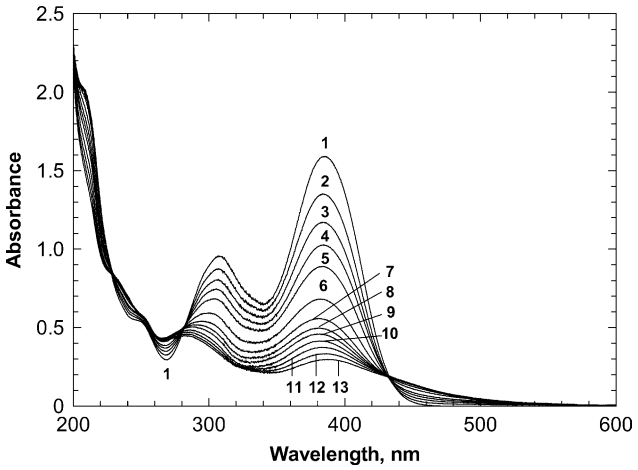

Fig. 5. Time-dependent absorption spectra of **3** in ACN ($\lambda_{irr} = 360$ nm; $I_0 = 4$ mW/cm^2): (1) 0 min; (2) 15 min; (3) 30 min; (4) 45 min; (5) 60 min; (6) 90 min; (7) 120 min; (8) 150 min; (9) 180 min; (10) 240 min; (11) 300 min; (12) 360 min; and (13) 420 min.

led to a dramatically increase in photostability of **1** ($\Phi \approx 2.7 \times 10^{-6}$). The concentration of the triplet oxygen, $^3O_2$, in ACN is 9.1×10^{-3} M [17], much larger than the concentration of **1**. Thus, it can be assumed that the concentration of any generated singlet oxygen $^1O_2$ may be comparable to the fluorene concentration and leads to the second-order of photoreaction. Therefore, it may be assumed that the photodegradation processes of **1** in ACN (at $\lambda_{irr} \approx 360$ nm and $C \approx 2.4 \times 10^{-5}$ M) are mainly determined by the $^1O_2$ concentration (self-oxidation process), in contrast to the unsubstituted fluorene which exhibited low efficiency in the reaction with $^1O_2$ [14].

Short wavelength excitation at $\lambda_{irr} \approx 250$ nm corresponds to the transitions into high excited electronic states of compounds **1**–**3** [7]. In this case, the quantum yield of the photoreaction of **1** decreased by 1.5–2 times and the influence of oxygen on the photodegradation process was reduced.

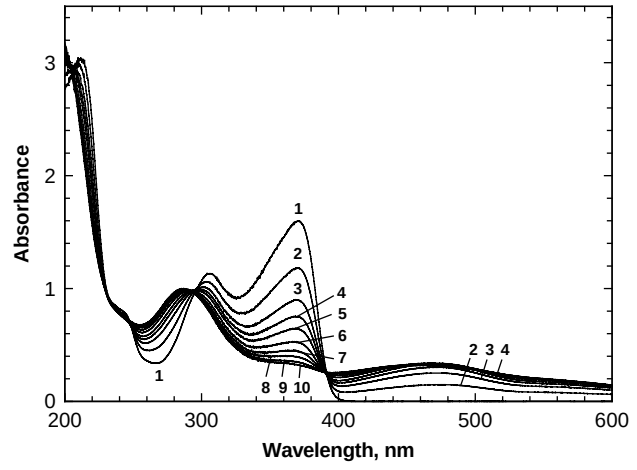

Fig. 4. Time-dependent absorption spectra of **2** in ACN ($\lambda_{irr} = 360$ nm; $I_0 = 4$ mW/cm^2): (1) 0 min; (2) 15 min; (3) 30 min; (4) 45 min; (5) 60 min; (6) 90 min; (7) 120 min; (8) 150 min; (9) 180 min; and (10) 210 min.

The absorption and fluorescence spectra of the photochemical products of **1** were nearly the same for $\lambda_{irr} \approx 360$ and $\lambda_{irr} \approx 250$ nm (Fig. 9). This means that the same mechanism of the photochemical decomposition of **1** occurred at both irradiation wavelengths, but different pathways resulted in population of the "photochemically active" electronic state. The fluorescence spectra of the photochemical products of **1** exhibited a dependence on the excitation wavelength. This can be explained by the formation of several fluorescent photoproducts in the spectral region 300–380 nm.

3.2. Analysis of **2**

Fluorene **2** is a symmetrical fluorene derivative bearing two diphenylamino substituents with strong electron-donating properties. Time-dependent absorption spectra of **2** upon irradiation at $\lambda_{irr} \approx 360$ nm are presented in Fig. 4. Values of Φ for different concentrations, oxygen content of the solvent, and its dependence on irradiation wavelength are presented in Table 1 and Fig. 7. As can be seen from the data in Table 1, the quantum yield of the photoreaction of **2** increased with concentration and exhibited complicated photochemical decomposition, including at least two different mechanisms. One possible mechanism involves generation and reaction of singlet oxygen (second-order photoreaction), while deoxygenation of the solvent led to an increase in photostability.

The second mechanism may be associated with an electron transfer process proceeding from the amine group with the formation of a stable cation radicals (first-order photoreaction) [18]. This mechanism is nearly independent of the oxygen concentration and is characterized by an increase in Φ under short wavelength excitation. Thus, the value of Φ for N_2-saturated solutions increased from 1.8×10^{-4} ($\lambda_{irr} \approx 360$ nm) to 5×10^{-4} ($\lambda_{irr} \approx 250$ nm). Cation radical

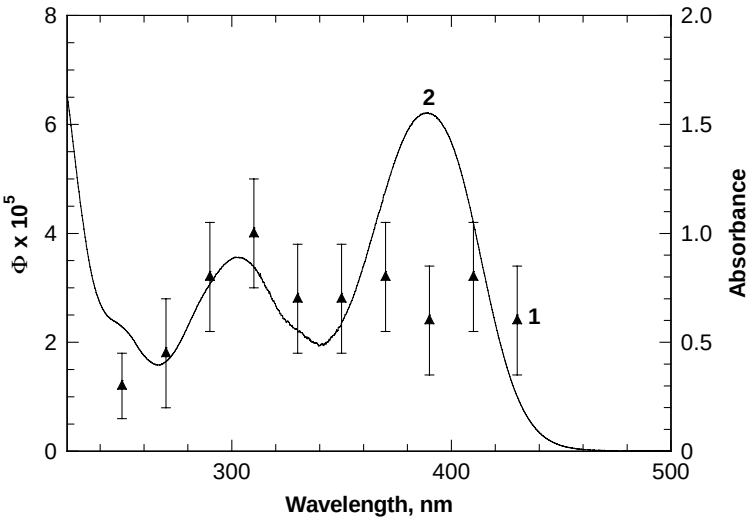

Fig. 6. Dependence of the photoreaction quantum yield, Φ: (1) on the irradiation wavelength for **1** in ACN and absorption spectrum of **1** in ACN.

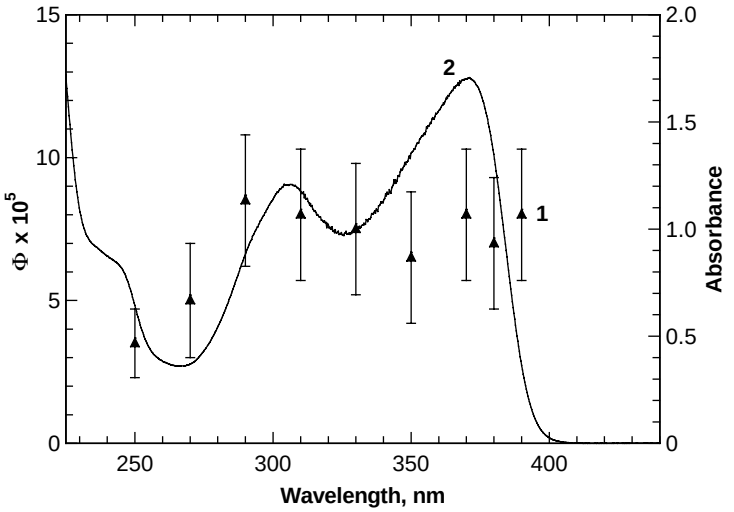

Fig. 7. Dependence of the photoreaction quantum yield, Φ: (1) on the irradiation wavelength for **2** in CAN and (2) absorption spectrum of **2** in ACN.

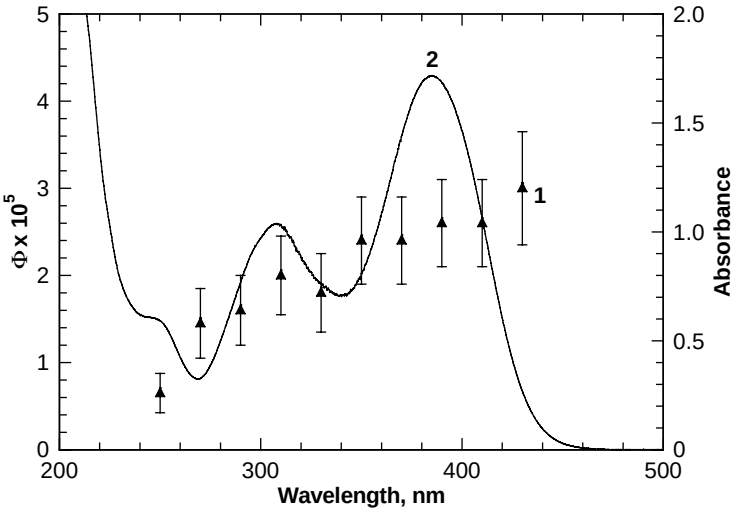

Fig. 8. Dependence of the photoreaction quantum yield, Φ: (1) on the irradiation wavelength for **3** in CAN and (2) absorption spectrum of **3** in ACN.

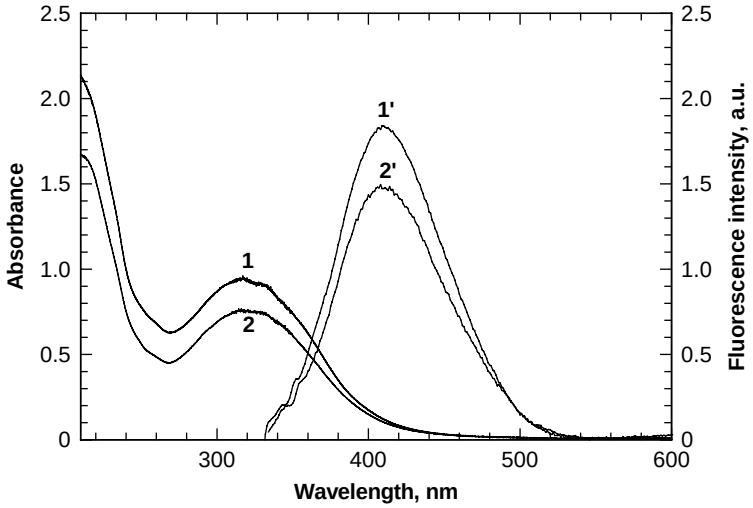

Fig. 9. Absorption (1, 2) and fluorescence spectra (1′, 2′, λ_{exc} = 320 nm) of the photochemical products of **1** in ACN after 120 min irradiation at λ_{irr} = 360 nm (1, 1′) and 120 min irradiation at λ_{irr} = 250 nm (2, 2′).

formation was also supported by the different absorption and fluorescence spectra of the photoproducts of **2** obtained at different irradiation wavelengths (Fig. 10). From Fig. 10 curves 1, 2, it can be seen that the composite absorption spectra of the photoproducts of **2** consists mainly of a short wavelength absorption, with maximum wavelength $\lambda_{max} \approx$ 290 nm, and a broad, long wavelength absorption band, with $\lambda_{max} \approx$ 430–460 nm. This latter absorption can be attributed to amine cation radicals [19].

The fluorescence spectra of the photoproducts of **2** (Fig. 10 curves 1′, 2′) are complex and depend on the excitation wavelength. Therefore, formation of a number of photoproducts occurred during irradiation. The excitation spectra of the photoproducts (Fig. 10 curves 1″ and 2″), whose fluorescence emission ranged from 430–530 nm (Fig. 10 curve 1′), were very similar to the absorption spectra of unsymmetrical fluorene derivatives **1** and **3** (Fig. 2 curves 1 and 3). Since the cation radical products are essentially nonfluorescent, these fluorescent photoproducts appear to be neutral species.

3.3. *Compound* **3**

Fluorene **3** also exhibited complex photochemical decomposition, dependent on concentration, oxygen content of the solution, and irradiation wavelength. Time-dependent absorption spectra of **3** for irradiation at $\lambda_{irr} \approx$ 360 nm and the wavelength dependence of the quantum yield of the photoreaction are presented in Fig. 5 and Fig. 8, respectively. A weak dependence of the quantum yield of the photoreaction of **3** on its concentration (see Table 1), indicating a high velocity constant for the first-order photoreaction. This

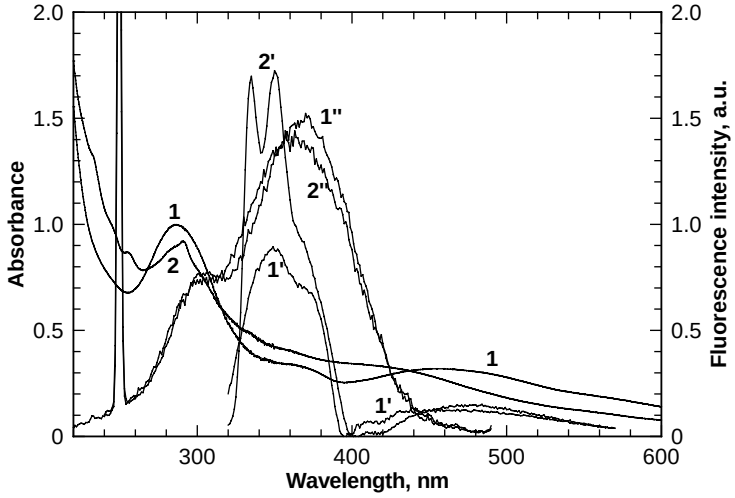

Fig. 10. Absorption (1, 2), fluorescence (1′, 2′, λ_{exc} = 290 nm), and excitation (1″, 2″, λ_{obs} = 500 nm) spectra of the photochemical products of **2** in ACN after 210 min irradiation at λ_{irr} = 360 nm (1, 1′, 1″) and 210 min irradiation at λ_{irr} = 250 nm (2, 2′, 2″).

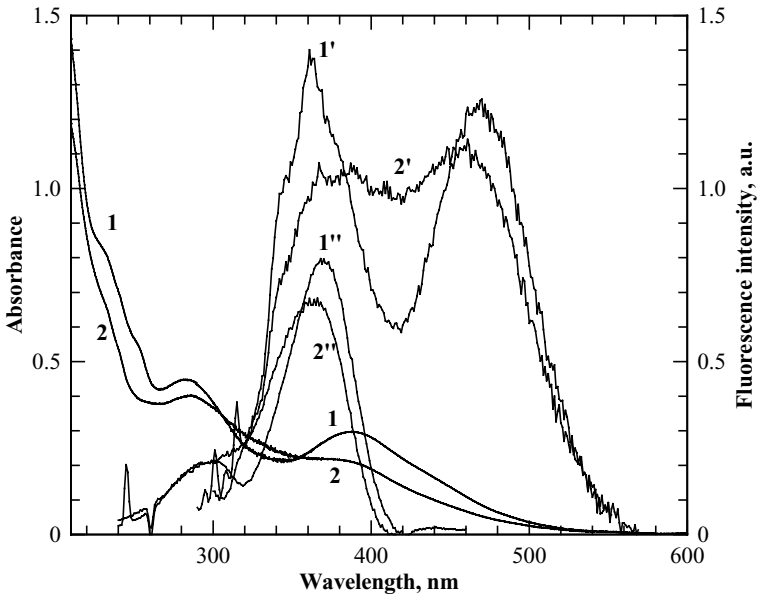

Fig. 11. Absorption (1, 2), fluorescence (1′, 2′, $\lambda_{exc} = 290$ nm), and excitation (1″, 2″, $\lambda_{obs} = 490$ nm) spectra of the photochemical products of **3** in ACN after 360 min irradiation at $\lambda_{irr} = 360$ nm (1, 1′, 1″) and 420 min irradiation at $\lambda_{irr} = 250$ nm (2, 2′, 2″).

first-order process played a dominant role and was strongly depended on oxygen content of the solvent. Assuming that the efficiency of the singlet oxygen formation is not efficient for **3** (since the fluorescence quantum yield of **3** in ACN $\sim$ 0.9 [7]), molecular $^3O_2$ oxygen is the primary reactant in this process. The role of $^3O_2$ should be important since its concentration in ACN is $\approx 9 \times 10^{-3}$ M compared to the concentration of **3** ($\leq 5 \times 10^{-5}$ M).

The quantum yield for the photoreaction for air-saturated solutions of all three derivatives decreased in the short wavelength region (see Table 1 and Figs. 6–8 for **1**–**3**, respectively). This result is unusual and further investigation is needed to understand the exact reason for this behavior. The photobleaching of N_2-saturated solutions of **3** was more efficient for short wavelength irradiation $\lambda_{irr} \approx 250$ nm.

The absorption and fluorescence spectra of the photoproducts of **3** are shown in Fig. 11, their complexity suggests a number of photochemical processes occurred. The excitation spectra (curves 1″, 2″) revealed the formation of neutral fluorene species exhibiting intense fluorescence emission from 460–500 nm. The photochemical decomposition of **3** was strongly dependent on molecular oxygen $^3O_2$. The electron transfer mechanism also occurred, resulting in photoproducts that absorb in the spectral region $\lambda \geq 440$ nm (Fig. 5, and Fig. 11, curves 1, 2).

4. Conclusions

The photochemical properties of a series of TPA fluorene derivatives **1**–**3** were investigated in ACN as a function of fluorene derivative concentration, oxygen content of the solvent, and irradiation wavelength. The quantum yields of the photoreactions of **1**–**3** in air saturated solutions decreased under excitation into higher excited electronic states ($\lambda_{irr} \approx$ 250 nm). For the N_2-saturated solutions, the opposite dependencies of Φ on the irradiation wavelength were observed. The analyses of the quantum yields of the photoreactions, along with the absorption and fluorescence spectra of the photoproducts, suggest the following mechanisms for the photodegradation of compounds **1**–**3**:

- singlet oxygen formation via sensitization by excited fluorene molecules, followed by bimolecular reaction between $^1O_2$ and the ground state fluorene derivative;
- direct molecular oxygen $^3O_2$ reaction with the excited fluorene derivative; and
- electron transfer processes with the formation of stable cation radicals (or other nonfluorescent photoproducts) with absorption at $\lambda \geq 440$ nm.

The photochemical decomposition of **1** was primarily influenced by singlet oxygen formation (second-order photoreaction) and decreased by over two-orders of magnitude when oxygen was excluded. Symmetrical fluorene derivative **2**, with two electron-donating diphenylamino groups, exhibited reactivity that can be largely attributed to photoreaction with singlet oxygen and electron transfer processes. The photostability of **3** was dependent on oxygen concentration in the solvent, suggesting a dominant role of molecular oxygen $^3O_2$ in the photoprocesses. The appearance of long wavelength absorption species also suggest an electron transfer process occurred in the photodegradation of **3**, resulting in formation of cation radical photoproducts. The low photochemical quantum yield ($\Phi \sim 10^{-4}$–10^{-6} in oxygen-free environments) suggests relatively high photostability of **1**–**3**. The photostability of the derivatives, along

with their high fluorescence quantum yields and two-photon absorptivity makes them particularly promising in nonlinear optical applications.

Acknowledgements

We wish to acknowledge the donors of The Petroleum Research Fund of the American Chemical Society, the Research Corporation Cottrell College Science program, the National Research Council COBASE award, the National Science Foundation, and the University of Central Florida Presidential Initiative for Major Research Equipment for partial support of this work.

References

[1] L.W. Tutt, T.F. Boggess, Prog. Quantum Electron. 17 (1993) 299–338.
[2] W. Denk, J.H. Strickler, W.W. Webb, Science 248 (1990) 73–76.
[3] E.A. Wachter, W.P. Partridge, W.G. Fisher, H.C. Dees, M.G. Petersen, Proc. SPIE Int. Soc. Opt. Eng. 3269 (1998) 68–75.
[4] K.D. Belfield, K.J. Schafer, Y. Liu, J. Liu, X. Ren, E.W. Van Stryland, J. Phys. Org. Chem. 13 (2000) 837–849.
[5] K.D. Belfield, D.J. Hagan, E.W. Van Stryland, K.J. Schafer, R.A. Negres, Org. Lett. 1 (1999) 1575–1578.
[6] K.D. Belfield, K.J. Schafer, W. Mourad, B.A. Reinhardt, J. Org. Chem. 65 (2000) 4475–4481.
[7] K.D. Belfield, M.V. Bondar, O.V. Przhonska, K.J. Schafer, W. Mourad, J. Lumin. 97 (2002) 141–146.
[8] G.S. He, L. Yuan, N. Cheng, J.D. Bhawalkar, P.N. Prasad, L.L. Brott, S.J. Klarson, B.A. Reinhardt, J. Opt. Soc. Am. B 14 (1997) 1079–1087.
[9] B.A. Reinhardt, L.L. Brott, S.J. Klarson, A.G. Dillard, J.C. Bhatt, R. Kannan, L. Yuan, G.S. He, P.N. Prasad, Chem. Mater. 10 (1998) 1863–1874.
[10] H.E. Pudavar, M.P. Joshi, P.N. Prasad, B.A. Reinhardt, Appl. Phys. Lett. 74 (1999) 1338–1340.
[11] J.W. Baur, J.M.D. Alexander, M. Banach, L.R. Denny, B.A. Reinhardt, R.A. Vaia, Chem. Mater. 11 (1999) 2899–2906.
[12] M.P. Ligocki, C. Leuenberger, J.F. Pankow, Atmos. Environ. 19 (1985) 1609–1617.
[13] R.M. Dickhut, K.E. Gustafson, Environ. Sci. Technol. 29 (1995) 1518–1525.
[14] L. Moeini-Nombel, S. Matsuzawa, J. Photochem. Photobiol. A: Chem. 119 (1998) 15–23.
[15] J.T. Barbas, M.E. Sigman, R. Arce, R.J. Dabestani, J. Photochem. Photobiol. A: Chem. 109 (1997) 229–236.
[16] K.D. Belfield, M.V. Bondar, Y. Liu, O.V. Przhonska, J. Phys. Org. Chem. 16 (2003) 69–78.
[17] S.L. Murov, I. Carmichael, G.L. Hug, Handbook of Photochemistry, Marcel Dekker, New York, 1993, p. 289.
[18] P.D. Wood, L.J. Johnston, J. Phys. Chem. A 102 (1998) 5585–5591.
[19] K.D. Belfield, M.V. Bondar, A.R. Morales, O. Yavuz, O.V. Przhonska, J. Phys. Org. Chem. 16 (2003) 194–201.